AAPS PharmSciTech (2019) 20: 264
DOI: 10.1208/s12249-019-1481-1

Research Article

Theme: Advances in Topical Delivery of Drugs
Guest Editor: S. Narasimha Murthy

Effects of Temperature and Humidity on the Skin Permeation of Hydrophilic and Hydrophobic Drugs

Hiroaki Iikura,[1] Koji Uchida,[1] Chie Ogawa-Fuse,[2] Kotatsu Bito,[3] Satoru Naitou,[1] Masaru Hosokawa,[1] Takashi Uchida,[1,4] Tomohiko Sano,[5,6] Hiroaki Todo,[4] and Kenji Sugibayashi[4,6]

Received 6 February 2019; accepted 12 July 2019; published online 24 July 2019

Abstract. The humidity was a well-known method to hydrate the skin; however, the published data were varied, and systemic experiments in the previous papers were few. Therefore, the *in vitro* permeation of excised porcine ear skin by drugs with different polarities [aminopyrine (AMP), antipyrine (ANP), methylparaben (MP), and ibuprofen (IP)] was analyzed under a constant skin surface temperature with different temperatures and humidities to reveal the effects of temperature and humidity on the skin permeation enhancement effects. Applied formulations were prepared by mixing the drug and a hydrophilic vehicle containing glycerin. The disposition-distance profiles of water and the humectant glycerin in the stratum corneum were also investigated using confocal Raman microscopy. High absolute humidity (AH) significantly contributed to the high skin penetration of the hydrophilic penetrants AMP, ANP, and MP but not the hydrophobic penetrant IP. An increase in the partition parameter and a decrease in the diffusivity parameter occurred with an increase in AH, independent of drug polarity. Moreover, we found that dew condensation induced by high AH on temperature-controlled skin surface may effectively increase water content and may provide higher glycerin distribution in the skin barrier, the stratum corneum. Increasing the amount of water and hydrophilic vehicles such as glycerin in the stratum corneum may enhance the permeation of hydrophilic penetrants AMP, ANP, and MP. These data suggested a dew condensation on the skin surface induced by high AH at a constant skin surface temperature would be important to enhance hydrophilic penetrants.

KEY WORDS: temperature; absolute humidity; skin permeation enhancement; dew condensation; hydrophilic and hydrophobic penetrants.

INTRODUCTION

The skin is the largest organ of the human body, located at the boundary between the body and the external environment. The stratum corneum, the outermost layer of the skin (10–20 μm thick), comprises dead keratinocytes embedded in a multilamellar lipid matrix, forming a "brick and mortar" structure. The stratum corneum often hinders the penetration of molecules through the skin (1). Therefore, numerous methods are utilized to enhance the delivery of active ingredients to local skin tissue, to the body *via* the systemic circulation, or both. This can be accomplished using lipid carriers (2), chemical penetration enhancers (3), and physical means, including iontophoresis (4), ultrasound (5), and microneedles (6). Furthermore, skin temperature modulation, through the application of heat, has the potential to temporarily and reversibly overcome the impermeability of penetrants by increasing drug diffusivity into the stratum corneum, increasing drug partitioning into the stratum corneum, disruption of lipid structures in the stratum corneum, or a combination of these (7).

Hydration of the skin using high humidity may enhance the skin permeability of penetrants. For example,

Guest Editor: S. Narasimha Murthy

[1] R&D–Development Research, Kao Corporation, 2-1-3 Bunka, Sumida-ku, Tokyo, 131-8501, Japan.
[2] Biological Science Laboratories, Kao Corporation, 2606 Akabane, Ichikai-machi, Haga-gun, Tochigi, 321-3497, Japan.
[3] Analytical Science Research Laboratories, Kao Corporation, 2606 Akabane, Ichikai-machi, Haga-gun, Tochigi, 321-3497, Japan.
[4] Faculty of Pharmacy and Pharmaceutical Sciences, Josai University, 1-1 Keyakidai, Sakado, Saitama, 350-0295, Japan.
[5] Faculty of Life and Environmental Sciences, Teikyo University of Science, 2-2-1 Senju Sakuragi, Adachi-ku, Tokyo, 120-0045, Japan.
[6] To whom correspondence should be addressed. (e–mail: sano-tmhk@ntu.ac.jpsugib@josai.ac.jp)

Lboutounne *et al*. found that increasing the relative humidity (RH) from 28 to 70% at 27°C led to a significant increase in + percutaneous absorption of caffeine (8). These analyses were performed using devices that control humidity and skin surface temperature on the donor side while the receptor fluid temperature was maintained at 37°C. Ishida *et al*. used a CO_2 chamber to show that the effect of humidity on the *in vitro* penetration of human skin by drugs increased the permeability coefficient (*P*) values of nicotine and isosorbide dinitrate at 95% RH and 32°C compared with those at 50% RH at 32°C (9). Furthermore, Chang and Reviere found that higher RH values on the donor side significantly increased the skin permeation of parathion at 37°C and 40°C. Moreover, they showed that varying temperatures and RH had independent effects on the skin permeation of parathion (10).

The application of high temperature and humidity may induce a marked effect on the skin permeation of drugs. Humidity-induced skin hydration could be a complicated phenomenon. Humidification on the donor side is generally related to skin hydration because dew condensation occurs on skin surface in conditions of high humidity. Skin surface temperature is changed by atmospheric temperature and humidity because of vaporization heat. Therefore, skin surface temperature should be controlled to evaluate effect of humidity on the skin permeation of applied drugs. In the present study, the temperature of the receiver solution was set to 32°C, independent of environmental conditions, and elucidation of the skin penetration enhancement effect was performed in different temperatures and humidity conditions with different drug polarities.

EXPERIMENTAL

Materials

The model drugs used for *in vitro* skin permeation experiments were as follows: antipyrine (ANP) (molecular weight [MW], 188; log $K_{o/w}$, − 1.51) (11), aminopyrine (AMP) (MW, 231; log $K_{o/w}$, 1.10) (12), methylparaben (MP) (MW, 152; log $K_{o/w}$, 1.93) (11), and ibuprofen (IP) (MW, 206; log $K_{o/w}$, 3.94) (12) were purchased from Tokyo Chemical Industry Co., Ltd. (Tokyo, Japan). 1,3-Propanediol (1,3-PD), 1,3-butanediol (1,3-BG), and dipropylene glycol (DPG) were from DuPont Tate & Lyle Bio Products Company, LLC (London, UK), DICEL Co. (Osaka, Japan), and Adeka Co. (Tokyo, Japan), respectively. Glycerin (Gly) and polyoxyethylene (60) hydrogenated castor oil (PEG60 CAS) were obtained from Kao Corp. (Tokyo, Japan). Deuterated water and deuterated glycerin were purchased from Cambridge Isotope Laboratories, Inc. (Andover, MA, USA) and C/D/N Isotopes, Inc. (Pointe-Claire, Quebec, Canada), respectively. Other regents and solvents were analytical grade and used without purification.

Preparation of Donor

Saturated solutions of ANP, AMP, MP, or IP were prepared for use in *in vitro* skin permeation experiments to compare permeability in conditions with equivalent thermodynamic activities, to perform the permeation experiments using a practical formulation, containing common ingredients such as the moisturizers: Gly, 1,3-PD, 1,3-BG, DPG, and the surfactant PEG60 CAS. Table I shows the composition of the vehicle solution. The solutions were prepared by mixing an excess amount of the drug with the vehicle (composed of moisturizers and surfactant) in practical formulations at 27°C or 40°C for approximately 3 h, according to the skin surface temperature. The supernatant was used as the saturated solution after passing it through a 0.45-μm disposable filter (Toyo Roshi Kaisha Ltd., Tokyo, Japan). The solubility of each drug at saturation was measured using high-performance liquid chromatography (HPLC).

Preparation of Skin

Porcine ear skin from Landrace-Yorkshire hybrids was obtained from Dard Co., Ltd. (Tokyo, Japan). These specimens were stored at − 30°C to preserve freshness. The frozen skin specimens, which were tightly packed by plastic bags, were thawed in warm water at 32°C for 30 min. After gently removing hair with a shaver (Lamdash ES-ST27, Panasonic Corp., Osaka, Japan), skin specimens were excised from the ears using a disposable surgical scalpel, and the subcutaneous fat was removed from each specimen. The thickness of the specimens was approximately 1.0–1.2 mm. Finally, the skin was cut into 2.5-cm squares. The skin pieces were used immediately to avoid spoilage (13).

Skin Permeation

The skin specimens were sandwiched between the receiver and donor chambers of a Franz diffusion cell (effective diffusion area, 1.77 cm^2; receiver and donor volumes, 6.0 and 5.0 ml, respectively). The receiver compartment was filled with phosphate-buffered saline (PBS), pH 7.4. The diffusion cells were equilibrated in a climate chamber (SH642; Espec Corp., Osaka, Japan), which simultaneously controlled temperature and humidity. The cells were placed on a stirring plate in the climate chamber. A small Teflon-coated magnetic bar was included in the receiver compartment and used to stir the sample to maintain the receiver fluid at a constant concentration and temperature (Fig. 1).

The permeation experiments included 1-h acclimation and then 8-h sampling periods (14). The permeation experiments were performed with conditions as follows: 48°C/95% RH, 50°C/55% RH, 52°C/30% RH, and 27°C/55% RH. The conditions are abbreviated as $T_{48}RH_{95}$, $T_{50}RH_{55}$, $T_{52}RH_{30}$, and $T_{27}RH_{55}$, respectively. The surface skin temperature was adjusted to 40°C when the environmental conditions were $T_{48}RH_{95}$, $T_{50}RH_{55}$, and $T_{52}RH_{30}$, whereas the skin temperature was 29°C for $T_{27}RH_{55}$. The reason for the different temperatures for 48°C/95% RH, 50°C/55% RH, and 52°C/30% RH was to maintain the skin surface temperature at 40°C, except for $T_{27}RH_{55}$. The changes in skin surface temperature and RH value in the chamber were monitored using a temperature humidity sensor (SHT7, Syscom Corp., Tokyo, Japan), and the data recorded using a logger (MSHT-16; Ymatic Inc., Tokyo, Japan). The receiver fluid was maintained at 32°C using circulating water (32°C) driven by a circulator (NCB-1200, Eyela Co. Ltd., Tokyo Japan), regardless of the environment conditions. Thus, the skin

Table I. Composition Ratios of the Vehicle

Composition ratio	PBS	Glycerin	1,3-PD	1,3-BG	DPG	PEG60 CAS
wt%	58	24	6.0	5.0	4.0	3.0

PBS phosphate-buffered saline; *1,3-PD* 1,3-propanediol; *1,3-BG* 1,3-butanediol; *DPG* dipropylene glycol; *PEG60 CAS* polyoxyethylene (60) hydrogenated castor oil

temperature reached 29°C in $T_{27}RH_{55\%}$ due to the circulating water. Furthermore, absolute humidity (AH) was calculated using the Tetens equation, as follows (15):

$$e(T) = 6.1078 \times 10^{\frac{7.5T}{(T+237.3)}} \quad (1)$$

$$\mathrm{AH}\left[\frac{\mathrm{g}}{\mathrm{m}^3}\right] = \frac{\text{Relative humidity}}{100} \times \frac{217 \times e(T)}{T + 273.15} \quad (2)$$

where $e(T)$ is the saturation vapor pressure and T is expressed as °C. Table II lists the experimental conditions used in the present study.

The donor solution for each model drug was stirred for 1-h at 40°C or 27°C according to the skin surface temperature before conducting the permeation experiment. The diffusion cell was equilibrated for 1-h for each environmental condition, followed by the addition of 1.0 ml of saturated donor solution to each donor cell. During the permeation study, 100 μl of receiver fluid was withdrawn every 1-h, and an equal volume of fresh PBS was added immediately. The receiver samples were analyzed using an HPLC system, as described below.

HPLC Measurements

HPLC measurements were carried out using a Hitachi HPLC system as follows: pump, L-2400; column oven, L-2300; autosampler, L-2200; and UV detector, L-2400. Each device was purchased from Hitachi Co., Ltd. (Tokyo, Japan).

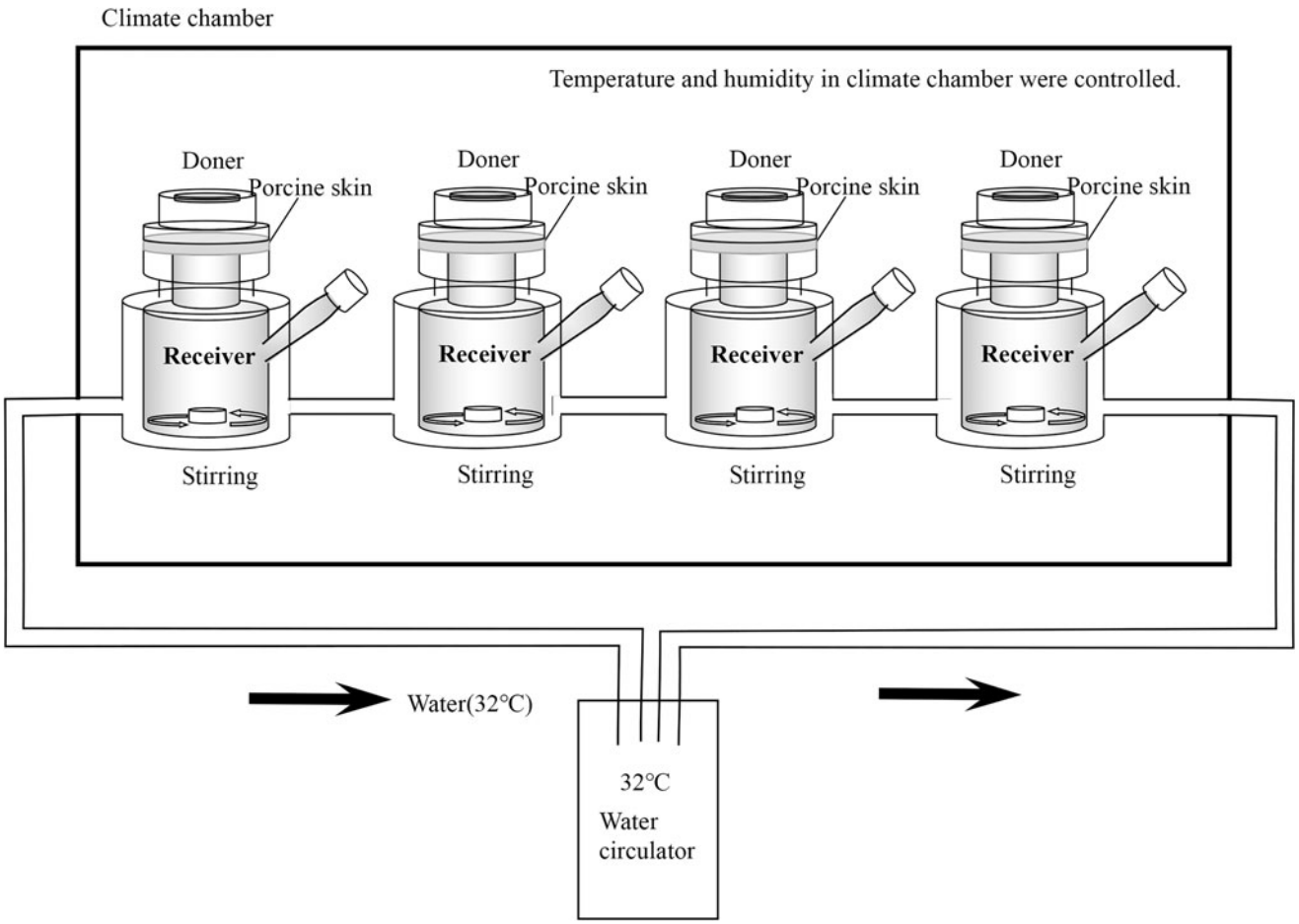

Fig. 1. Illustration of skin permeation system, which can maintain environmental temperature, humidity, and skin surface temperature at the same time

Table II. Experimental Conditions

Experimental condition	Temperature (°C)	Relative humidity (% RH)	AH (g/m^3)	Skin surface temperature (°C)
$T_{48}RH_{95}$	48	95	71.7	40
$T_{50}RH_{55}$	50	55	45.6	40
$T_{52}RH_{30}$	52	30	27.3	40
$T_{27}RH_{55}$	27	55	14.2	29

An Inertsil ODS-3 (GL Science Inc., Tokyo, Japan) was used as the HPLC column and was maintained at 40°C in the oven. The drugs were dissolved in PBS to standard concentrations, and the samples were appropriately diluted with distilled water to the measurement range of the HPLC. The flow rate and injection volume were 1 ml/min and 20 μl, respectively. The mobile phase compositions and detection UV wavelengths were as follows: 10% acetonitrile (HPLC grade, Wako Chemical Co., Ltd., Osaka, Japan) and 90% distilled water (HPLC grade, Wako Chemical Co., Ltd.), 254 nm for ANP; 3% acetonitrile with 97% distilled water containing 0.1% phosphoric acid (Kanto Chemical Co., Inc., Tokyo, Japan), 245 nm for AMP; 30% methanol and 70% distilled water, 254 nm for MP; and 45% acetonitrile and 55% distilled water containing 20 mM phosphoric acid, 230 nm for IP.

Data Analysis

The receiver solution was sampled hourly for 8-h after 1-h acclimation. The cumulative amount of drug, Q (μg/cm^2), that permeated through the skin per unit area for effective diffusion was plotted against time. The linear portion of the plot (five successive data points) was designated steady-state flux (J_{ss}). Lag time (t_{lag}) was calculated from the intercept, $Q = 0$, of the straight line to determine J_{ss}. The permeability coefficient (P) was defined as

$$P = \frac{J_{ss}}{C_v} \tag{3}$$

where C_v is the drug concentration in the donor solution. P is a criterion of the permeation capacity of a certain penetrant. Furthermore, Flynn *et al.* and Okamoto *et al.* determined the partition (KL) and diffusion (DL^{-2}) parameters using Fick's law of diffusion as follows (16,17):

$$KL = PL^2/D \tag{4}$$

$$D/L^2 = 1/6t_{lag,} \tag{5}$$

where L represents the thickness of the skin barrier. L may be difficult to accurately calculate using skin permeation data similar to those presented here. Therefore, KL and DL^{-2} are frequently calculated. Although using these parameters assumes that the skin is a uniform membrane, these parameters partially describe penetration behavior. Furthermore, the skin penetration enhancement ratio (ER) was calculated from the ratio of the experimental P value to that obtained using $T_{27}RH_{55}$.

Confocal Raman Microspectroscopy

Confocal Raman microspectroscopy was used to determine the characteristics of the stratum corneum, such as the distribution of water and drugs (18,19). In the present study, changes in the water content of the stratum corneum were initially measured using different conditions. Moreover, penetration into the stratum corneum by glycerin in the vehicle was investigated to determine the effect of solvent.

Water Distribution

The skin was mounted in the Franz-typed diffusion cells and acclimated for 1-h in the climate-controlled chamber. The receiver fluid was maintained at 32°C by circulating the water (32°C) through a water jacket. The skin was mounted onto the sample stage of a confocal Raman microspectrometer (Nanofinder 30; Tokyo Instruments, Inc., Tokyo, Japan) for 1 h after acclimation. Water distribution was calculated from the Raman signal ratio of the OH stretch bands of water (3100–3750 cm^{-1}) to the CH stretch bands of proteins (2800–3000 cm^{-1}). Furthermore, before acclimation, the water content of skin was measured as the initial distribution of water at $T_{23}RH_{50}$ (ambient temperature and humidity where confocal Raman microspectrometer was placed). All measurements were performed five times ($n = 3$ for each condition).

Glycerin Penetration

Deuterated water or the mixed vehicle (60% deuterated water and 40% d5-1,1,2,3,3-glycerin) was applied to the skin for 1 h after acclimation at $T_{52}RH_{30}$ and $T_{48}RH_{95}$. After 1 h more, the distribution of glycerin in the stratum corneum was measured using a Nanofinder Flex confocal Raman microspectroscopy system.

The deuterated glycerin content was calculated from the Raman signal ratio of the CD stretch bands of deuterated glycerin (2000–2275 cm^{-1}) to the CH stretch bands of proteins (2800–3000 cm^{-1}). The proprietary acquisition software (Nanofinder ver. 8.0, Tokyo Instruments, Inc. and Igor Pro 6.1, WaveMetrics, Inc., OR, USA) supplied with the instrument used spectral analysis. All measurements were performed five times ($n = 3$ for each condition).

Statistical Analysis

The data represent the mean values ($n \geq 4$) ± standard deviation, unless stated otherwise. Permeability data were rejected only when unreasonably high solute permeability flux was observed.

Statistical analysis was performed using Microsoft Excel software. Student's t test was performed, and significant differences were defined as $P \leq 0.05$.

RESULTS

The Effects of Temperature and Humidity on the Skin Penetration of Drugs

Figure 2a, b shows the cumulative amount of IP and ANP that permeated through the skin at different temperatures and humidities, respectively. Here, IP and ANP were selected as model nonpolar and polar penetrants, respectively. The ordinate of the graph represents the cumulative amount of the drugs that permeated per unit diffusion area of the skin, Q (μg/cm^2). The Q values of IP at $T_{48}RH_{95}$, $T_{50}RH_{55}$, and $T_{52}RH_{30}$ (40°C, skin surface temperature) were higher compared with those at $T_{27}RH_{55}$ (29°C, skin surface temperature; Fig. 2a). In contrast, similar Q values of IP were obtained at $T_{48}RH_{95}$, $T_{50}RH_{55}$, and $T_{52}RH_{30}$, and the Q values of IP at a skin surface temperature 40°C were not much different compared.

The Q values of ANP at 40°C were higher compared with that at $T_{27}RH_{55}$ and were the same as the Q values of IP application (Fig. 2b). However, the Q values of ANP increased with increasing AH (RH).

Table III and Fig. 3a, b show the calculated skin permeation parameters of P (or log P), DL^{-2}, and the KL values *versus* those of the skin permeation profiles of IP and ANP in different experimental conditions. There were small but significant increases in P for IP at $T_{50}RH_{55}$ and $T_{52}RH_{30}$; furthermore, there were similar ER values of IP measured at $T_{48}RH_{95}$, $T_{50}RH_5$, and $T_{52}RH_{30}$ (1.28, 1.38, and 1.34 respectively). In contrast, the P values for ANP at $T_{48}RH_{95}$, $T_{50}RH_{55}$, and $T_{52}RH_{30}$ were clearly different. The ER values of ANP at $T_{48}RH_{95}$, $T_{50}RH_{55}$, and $T_{52}RH_{30}$ were 4.70, 3.73, and 1.70, respectively. Different skin penetration enhancement effects caused by changes in experimental conditions were observed for the skin permeation of IP and ANP. Therefore, the values of KL and DL^{-2} were further compared to clarify the effect of humidification on skin permeation.

Figure 4a, b shows the effects of humidification on the KL and DL^{-2} values of IP and ANP, respectively. Table III summarizes the calculated values. The DL^{-2} value of IP decreased with increasing AH values, and the KL value of IP increased as the AH value increased. The DL^{-2} value of IP at 71.7 AH ($T_{48}RH_{95}$) was 0.54 times smaller compared with that at 27.3 AH ($T_{52}RH_{30}$), whereas the KL value of IP at 71.7 AH was 1.73 times higher compared with that at 27.3 AH. In contrast, the DL^{-2} value of ANP slightly decreased although the KL value clearly increased when the AH value increased. The ER of the DL^{-2} value of ANP at 71.7 AH *versus* 27.3 AH was 0.80, whereas the KL value of ANP at 71.7 AH was 3.44 times higher than that at 27.3 AH.

Permeation Behaviors of AMP and MP

To further investigate the relationship between the polarity of the drugs and humidity, AMP and MP were analyzed. Figure 5 shows the relationship between log P values of the penetrants at $T_{48}RH_{95}$ and $T_{27}RH_{55}$ as well as their log $K_{o/w}$ values. At $T_{27}RH_{55}$, a linear correlation was observed between the log P and log $K_{o/w}$ values. In contrast, at $T_{48}RH_{95}$, log P increased linearly with increasing log $K_{o/w}$ values, until the value was < 2, although it was not different at $T_{48}RH_{95}$ and $T_{27}RH_{55}$ when the log $K_{o/w}$ value was 3.94 (IP).

Distribution of Water in the Stratum Corneum

Water distribution in the stratum corneum was measured using confocal Raman microscopy at $T_{48}RH_{95}$, $T_{52}RH_{30}$, and $T_{23}RH_{50}$. Figure 6 shows the distribution of water as a function of the depth of the stratum corneum. The water distribution at a shallow depth at $T_{48}RH_{95}$ was much higher compared with that at $T_{52}RH_{30}$ and $T_{23}RH_{50}$. Notably, the water distribution profile in the stratum corneum at $T_{52}RH_{30}$ did not differ compared with that at $T_{23}RH_{50}$.

Distribution of Glycerin in the Stratum Corneum

As an index of penetration of the vehicle component, the distribution of d5-glycerin in the stratum corneum was analyzed using a confocal Raman microscope. Figure 7 shows the depth profile of d5-glycerin in the stratum corneum. The distribution of d5-glycerin in the stratum corneum at $T_{48}RH_{95}$ was much higher compared with that at $T_{52}RH_{30}$, particularly at shallow depths.

DISCUSSION

Several reports have shown that application of high temperature and humidity increases the skin permeation of topically applied drugs (8–10,20,21). However, the results are likely to depend on their hydration methods. Here, we used a special chamber to determine the effects of high temperature and humidity on skin permeation *in vitro*.

In a preliminary experiment, we found that skin capacitance measured using a Corneometer (Cutometer® MPA 580 and Corneometer CM825 Courage+Khazaka electronic GmbH, Koln, Germany) was not increased after a 1-h acclimation at 95% RH and 40°C. We did not use a temperature control system in the receiver solution; therefore, the temperature of both environment and skin surface should be the same.

In contrast, using a receiver temperature control system to maintain at 32°C, which was lower than the temperature of the environment, a significant increase in the capacitance value in the same conditions was measured. Skin capacitance is related to skin hydration (22). Water vapor condensation occurs on the skin surface when the surface temperature is lower than the dew point temperature. Amount of saturated water vapor at 40°C is about 51.1 g/m^3 and that at 32°C is about 33.8 g/m^3 calculated using the Tetens equation (Eqs. 1 and 2). The AH values at $T_{48}RH_{95}$, $T_{50}RH_{55}$, and $T_{52}RH_{30}$ were 71.7 g/m^3, 45.6 g/m^3, and 27.3 g/m^3, respectively (Table II). Therefore, water vapor condensed on the skin

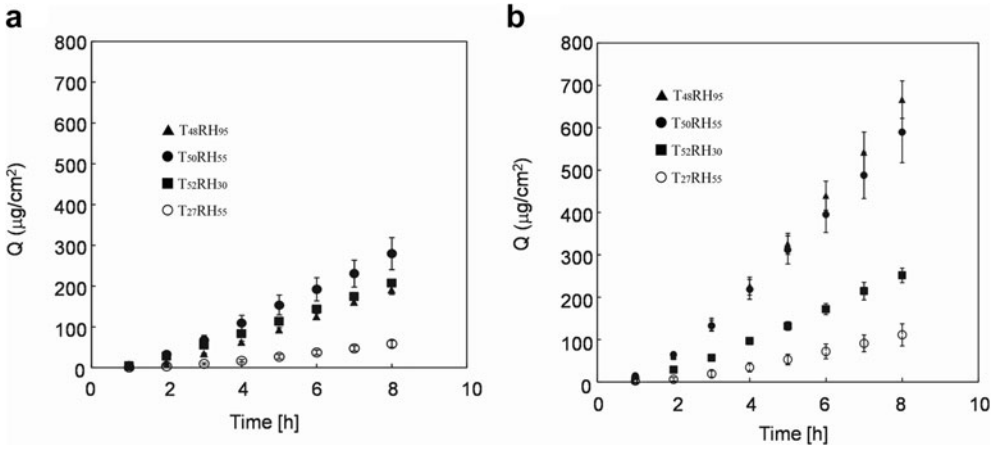

Fig. 2. Time course of the cumulative amounts (Q) of IP (**a**) and ANP (**b**) that permeated through excised porcine skin after 1-h acclimation under different environmental conditions. Preset conditions were as follows: $T_{48}RH_{95}$ (black triangle), $T_{50}RH_{55}$ (black circle), $T_{52}RH_{30}$ (black square), and $T_{27}RH_{55}$ (white circle). Each data point represents the mean ± SE (SE stands for standard error) ($n \geq 3$)

surface, if the temperatures of the skin surface and the receiver solution maintained at 32°C. We reasoned that these conditions may represent a key factor that influences the skin penetration-enhancing effect of topically applied drugs at high humidity and temperature in *in vitro* skin permeation experiments. Thus, in the present study, we conducted *in vitro* experiments using a climate chamber that maintained the reservoir solution temperature at 32°C independent of environmental conditions (Fig. 1).

High AH significantly contributed to the high skin penetration of the hydrophilic penetrants AMP, ANP, and MP but not the hydrophobic penetrant IP. An increase in the partitioning parameter and a decrease in the diffusivity parameter occurred with an increase in AH, independent of drug polarity (Figs. 2, 3, 4, and 5). A higher water and glycerin distribution-distance profile in the stratum corneum was observed using confocal Raman microscopy after a 1-h acclimation at $T_{48}RH_{95}$ compared with those at $T_{52}RH_{30}$ and $T_{23}RH_{50}$ (Figs. 6 and 7).

Temperature can modify the structure of the stratum corneum. Several thermal transitions of the stratum corneum have been identified at about 10°C, 35–40°C, 65–75°C, and 100°C. The transition at 35–40°C is small and reversible and is associated with lipids (23,24). The main lipid transitions of the stratum corneum appear at over 40°C, which may disturb the lamella structure and result in faster permeation (7). Mitragottori *et al.* found Arrhenius relationships between steady-state flux through porcine and human skin at application temperatures of 28–46°C. Furthermore, the phase transition from orthorhombic to hexagonal phases occurs in lipid structures in the stratum corneum at skin temperatures of 40°C (25).

Hydration of the stratum corneum can lead to structural rearrangement of lipids in corneocytes and increase the solubility of a penetrant in and through the stratum corneum (26). Vyumvuhore *et al.* investigated that the hydration of stratum corneum by Raman spectroscopy with various humidity levels at 20°C. They demonstrated that the intensities of sub-bands at 3280 cm^{-1} and 3345 cm^{-1}, which were assigned to partially bound water, did not vary between 4 and 28% RH, and then, it rose sharply before decreasing over 60%. A small band around 3470 cm^{-1}, which was assigned to unbound water, increased slightly up to 44% RH. Over 60% RH, the integrated intensity of the band increased significantly and proportionally with relative humidity. They suggested that unbound water that increased in the stratum corneum could interact with the polar heads of stratum corneum lipids and lead to a decrease in hydrogen bonding forces of the partially bound water and modify the spaces between hydrocarbon chains (27).

We assumed that water vapor with a high temperature might change the lipid structure in the stratum corneum and result in acceleration of hydration of the stratum corneum (28,29). Of note, higher amounts of glycerin were detected

Table III. Skin Permeation Parameters of IP and ANP

Penetrant	Environment condition	Log P	DL^{-2} ($\times 10^{-5}$) (1 s)	KL ($\times 10^{3}$) (cm)
IP	$T_{48}RH_{95}$	− 6.04 ± 0.048	2.22 ± 0.20	41.4 ± 7.28
	$T_{50}RH_{55}$	− 6.01 ± 0.046	3.12 ± 0.43	32.2 ± 7.48
	$T_{52}RH_{30}$	− 6.02 ± 0.053	4.13 ± 0.67	24.0 ± 7.20
	$T_{27}RH_{55}$	− 6.15 ± 0.089	1.95 ± 0.38	37.2 ± 7.57
ANP	$T_{48}RH_{95}$	− 7.35 ± 0.041	2.33 ± 0.14	1.93 ± 0.13
	$T_{50}RH_{55}$	− 7.46 ± 0.098	2.87 ± 0.23	1.26 ± 0.40
	$T_{52}RH_{30}$	− 7.79 ± 0.046	2.90 ± 0.22	0.56 ± 0.021
	$T_{27}RH_{55}$	− 8.03 ± 0.092	2.07 ± 0.18	0.46 ± 0.068

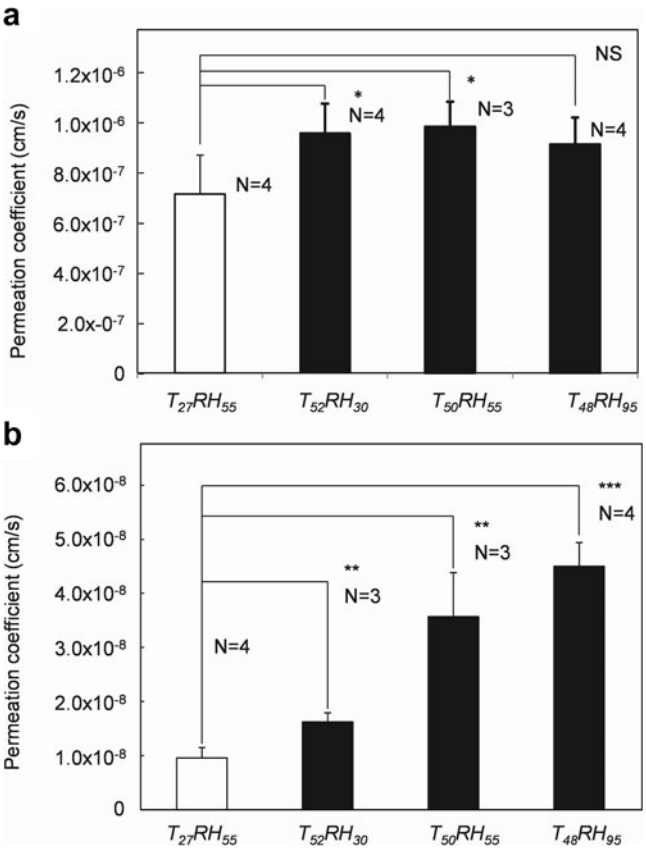

Fig. 3. Effects of humidification and temperature on the permeability coefficient (P) of IP (**a**) and ANP (**b**). The open and closed columns represent data at different skin surface temperatures, 27°C and 40°C, respectively. Each column represents the mean ± SE ($n \geq 3$). ***$P < 0.001$, **$P < 0.01$, *$P < 0.05$. NS no significant

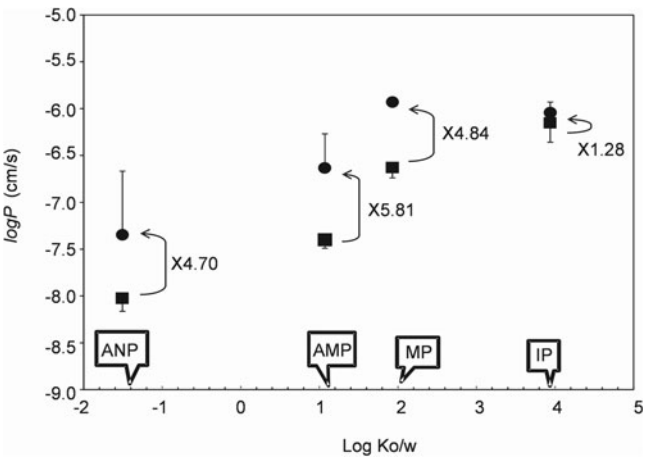

Fig. 5. Effects of humidification on the logarithm of the permeability coefficient (log P) of IP, MP, AMP, and ANP with different polarities. Symbols: black circle and black square: log P of the penetrants at $T_{48}RH_{95}$ and $T_{27}RH_{55}$, respectively. Each data point represents the mean ± SE ($n \geq 3$). The numbers in the figure indicate the enhancing ratio of P value at $T_{48}RH_{95}$ to that at $T_{27}RH_{55}$ of each drug

after the topical application of the formulation at $T_{48}RH_{95}$ compared with $T_{52}RH_{30}$. Swelling of the stratum corneum caused by an increase in the volume of water, glycerin concentration, or both would increase the thickness of the stratum corneum (30). Björklund *et al*. reported that glycerol and urea penetrate the skin membrane and can maintain the skin permeability characteristics associated with a hydrated skin membrane (31).

We used a mixed solvent in the present study so that the solvent in the formulation might affect skin permeation of the drugs by modifying the lipid structures in the stratum corneum. Further study is required to identify the solvent effect that enhances skin permeation at high humidity and temperature.

Although it was very difficult here to distinguish the skin penetration-enhancing effect of the application of high heat and humidity, the effect of a 1-h acclimation on skin permeation parameters was investigated using drugs with different lipophilicities. For example, the P value of the hydrophilic drug ANP increased in concert with an increase in the AH value, with an approximately 3.5 times higher KL value at $T_{48}RH_{95}$ (AH; 71.7 g/m^3) compared with that at $T_{52}RH_{30}$ (AH; 27.3 g/m^3). In contrast, the DL^{-2} value decreased slightly with an increase in the AH value. On the other hand, the extent of the change in KL and DL^{-2} values

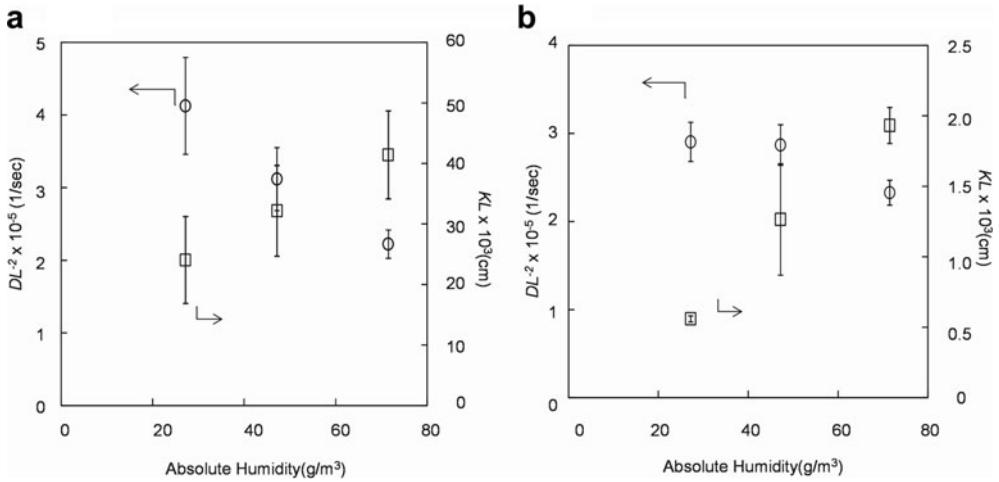

Fig. 4. Effects of humidification on the diffusion parameter (DL^{-2}) (white circle) and partition parameter (KL) (white square) calculated from the skin permeation profiles of IP (**a**) and ANP (**b**) at a skin surface temperature of 40°C. Each data point represents the mean ± SE ($n \geq 3$)

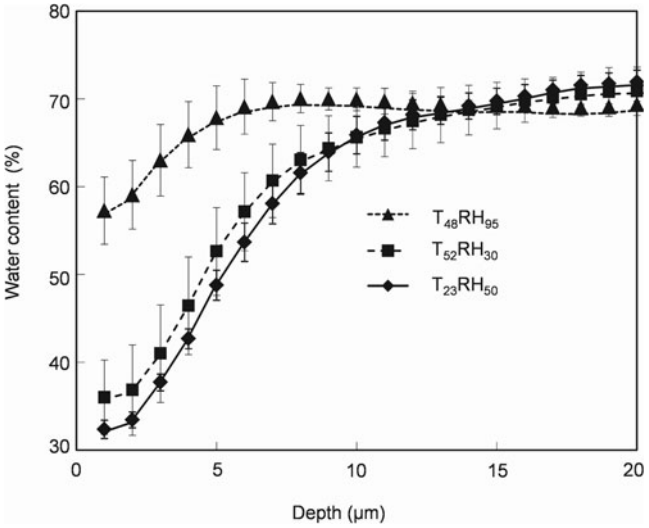

Fig. 6. Water content depth profiles in the stratum corneum of acclimatized skin in various environments. Temperature and humidity were as follows: $T_{48}RH_{95}$ (black triangle), $T_{52}RH_{30}$ (black square), and $T_{23}RH_{50}$ (black diamond). Each data point represents the mean ± SE ($n = 3$)

of the lipophilic drug IP differed compared with that of ANP, although we observed the same tendency for an increase and decrease in KL and DL^{-2} values, respectively.

Swelling of a lipid bilayer and the phase transition of a lipid structure in the stratum corneum due to increasing unbound water and glycerin may be related to the partition and diffusion parameters of topically applied drugs. Partitioning of a hydrophilic drug may be strongly influenced by these changes. Thus, 4.70-, 5.81-, and 4.84-fold higher permeation was observed for ANP, AMP, and MP, respectively, at $T_{48}RH_{95}$ compared with that at $T_{27}RH_{55}$, which may be caused by an increase in the KL value and a decrease in the DL^{-2} value. In contrast, the skin penetration-enhancing effect following acclimation to heat, and humidity would be ineffective for highly lipophilic drug such as IP, because the

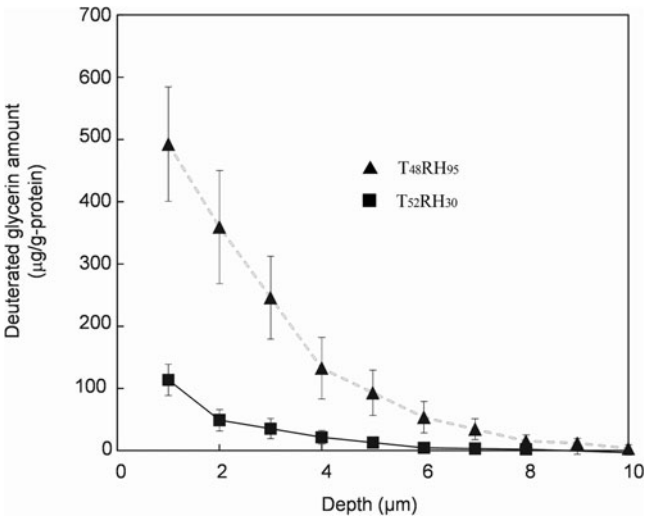

Fig. 7. d5-Deuterated glycerin depth profiles in the stratum corneum of acclimatized skin in several environments. Temperature and humidity were as follows: $T_{48}RH_{95}$ (black triangle) and $T_{52}RH_{30}$ (black square). Each data point represents the mean ± SE ($n = 3$)

increase in the KL value and the decrease in DL^{-2} value were similar to the increase in the AH value. Furthermore, no influence on ER was detected by the application of heat for IP permeation when P values were compared at $T_{48}RH_{95}$ and $T_{27}RH_{55}$.

Yosef *et al* reported the hydration effect on the permeation of salicylate esters, including methyl salicylate (log P, 2.55), ethyl salicylate (log P, 3.0), and glycol salicylate (log P, 1.63). They demonstrated that the enhancement ratios (steady-state flux of hydration *versus* steady-state flux of dehydration) of methyl salicylate, ethyl salicylate, and glycol salicylate solutions were 2.32, 2.26, and 1.98 respectively. They also suggested that the enhancements were mainly due to increased diffusivity of the salicylate esters in the stratum corneum. The hydration increased the flux of neat glycol salicylate 10-fold due to hygroscopic effect (32). In our study, the enhancement ratios of permeability constants of MP (log P, 1.93) and IP (log P, 3.94) at $T_{48}RH_{95}$ *versus* that at $T_{27}RH_{55}$ were 4.84 and 1.28, respectively. It may be difficult to compare both results directly due the difference in hydration method; however, both studies suggested that hygroscopic effects may influence the ability of hydration.

Further experiments should be conducted to evaluate the change in lipid structure and the thickness of the stratum corneum to identify the detailed mechanism of the effects of the application of heat and humidity to the skin. Thus, the application of heat at high AH may serve as an effective method to enhance skin permeation for hydrophilic to moderately lipophilic drugs as well as for water and a humectant such as glycerin.

CONCLUSIONS

The present study revealed that humidification of the stratum corneum by high humidity in a controlled environmental and skin temperature greatly contributed to the enhanced skin penetration of hydrophilic penetrants such as ANP, AMP, and MP. Confocal Raman spectroscopy measurements suggested that hydration caused by vapor condensation on the stratum corneum as well as a higher distribution of humectant and water represent important factors that enhance the skin permeation of drugs.

Moderate hydration and heat are considered to induce reversible structural changes in the lipid structure of the stratum corneum, which provides the homeostatic nature of protection provided by the skin. We conclude that humidification applied here may serve as an effective tool to enhance the skin permeation of hydrophilic penetrants while retaining the homeostatic nature of the stratum corneum.

REFERENCES

1. Barbero AM, Frasch HF. Effect of stratum corneum heterogeneity, anisotropy, asymmetry and follicular pathway on transdermal penetration. How sensitive are transdermal transport predictions by microscopic stratum corneum models to geometric and transport parameter input? J Control Release. 2017;260(1873–4995 (Electronic):234–46.
2. Schreier H, Bouwstra J. Liposomes and niosomes as topical drug carriers: dermal and transdermal drug delivery. J Control Release. 1994;30(1):1–15.

3. Lane ME. Skin penetration enhancers. Int J Pharm. 2013;447(1–2):12–21.
4. Guy RH, Delgado-Charro Mb Fau - Kalia YN, Kalia YN. Iontophoretic transport across the skin. Skin Pharmacol Appl Ski Physiol. 2001;14 Suppl1(1422–2868 (Print)):35–40.
5. Mitragotri S. Effect of therapeutic ultrasound on partition and diffusion coefficients in human stratum corneum. J Control Release. 2001;71(1):23–9.
6. van der Maaden K, Jiskoot W, Bouwstra J. Microneedle technologies for (trans)dermal drug and vaccine delivery. J Control Release. 2012;161(2):645–55.
7. Shahzad Y, Louw R, Gerber M, Du Plessis J. Breaching the skin barrier through temperature modulations. J Control Release. 2015;202:1–13.
8. Lboutounne Y, Silva J, Pazart L, Bérard M, Muret P, Humbert P. Microclimate next to the skin: influence on percutaneous absorption of caffeine (ex-vivo study). Skin Res Technol. 2014;20(3):293–8.
9. Ishida M, Takeuchi H, Endo H, Yamaguchi J-I. Impact of humidity on in vitro human skin permeation experiments for predicting in vivo permeability. J Pharm Sci. 2015;104(12):4223–31.
10. Chang SK, Riviere JE. Percutaneous absorption of parathion in vitro in porcine skin: effects of dose, temperature, humidity, and perfusate composition on absorptive flux. Fundam Appl Toxicol. 1991;17(3):494–504.
11. Uchida T, Yakumaru M, Nishioka K, Higashi Y, Sano T, Todo H, et al. Evaluation of a silicone membrane as an alternative to human skin for determining skin permeation parameters of chemical compounds. Chem Pharm Bull. 2016;64(9):1338–46.
12. Hatanaka T, Inuma M, Sugibayashi K, Morimoto Y. Prediction of skin permeability of drugs: I: comparison with artificial membrane. Chem Pharm Bull. 1990;38(12):3452–9.
13. Celebi D, Guy RH, Edler KJ, Scott JL. Ibuprofen delivery into and through the skin from novel oxidized cellulose-based gels and conventional topical formulations. (1873–3476 (Electronic)).
14. Zhang J, Michniak-Kohn B. Investigation of microemulsion microstructures and their relationship to transdermal permeation of model drugs: ketoprofen, lidocaine, and caffeine. Int J Pharm. 2011;421(1):34–44.
15. Tetens O. Uber einige meteorologische Begriffe. Z Geophys. 1930;6:297–309.
16. Flynn GL, Yalkowsky SH, Roseman TJ. Mass transport phenomena and models: theoretical concepts. J Pharm Sci. 1974;63(4):479–510.
17. Okamoto H, Hashida M, Sezaki H. Structure-activity relationship of 1-alkyl- or 1 -alkenylazacycloal kanone derivatives as percutaneous penetration enhancers. J Pharm Sci. 1988;77(5):418–24.
18. Albèr C, Brandner BD, Björklund S, Billsten P, Corkery RW, Engblom J. Effects of water gradients and use of urea on skin ultrastructure evaluated by confocal Raman microspectroscopy. Biochim Biophys Acta Biomembr. 2013;1828(11):2470–8.
19. Mateus R, Abdalghafor H, Oliveira G, Hadgraft J, Lane ME. A new paradigm in dermatopharmacokinetics—confocal Raman spectroscopy. Int J Pharm. 2013;444(1–2):106–8.
20. Fritsch WC, Stoughton RB. The effect of temperature and humidity on the penetration of C14 acetylsalicylic acid in excised human skin. J Investig Dermatol. 1963;41:307–11.
21. Idson B. Hydration and percutaneous absorption. Curr Probl Dermatol. 1978;7:132–41.
22. Clarys P, Clijsen R, Taeymans J, Barel AO. Hydration measurements of the stratum corneum: comparison between the capacitance method (digital version of the Corneometer CM 825®) and the impedance method (Skicon-200EX®). Skin Res Technol. 2012;18(3):316–23.
23. Golden GM, Guzek DB, Harris RR, McKie JE, Potts RO. Lipid thermotropic transitions in human stratum corneum. J Investig Dermatol. 1986;86(3):255–9.
24. Cornwell PA, Barry BW, Bouwstra JA, Gooris GS. Modes of action of terpene penetration enhancers in human skin; differential scanning calorimetry, small-angle X-ray diffraction and enhancer uptake studies. Int J Pharm. 1996;127(1):9–26.
25. Mitragotri S. Temperature dependence of skin permeability to hydrophilic and hydrophobic solutes. J Pharm Sci. 2007;96(0022–3549 (Print)):1832–9.
26. Bouwstra JA, de Graaff A, Gooris GS, Nijsse J, Wiechers JW, van Aelst AC. Water distribution and related morphology in human stratum corneum at different hydration levels. J Investig Dermatol. 2003;120(5):750–8.
27. Vyumvuhore R, Tfayli A, Duplan H, Delalleau A, Manfait M, Baiilet-Guffroy A. Effects of atmospheric relative humidity on stratum corneum structure at the molecular level: ex vivo Raman spectroscopy analysis. Analyst. 2013;138(14):4103–11.
28. Mitragotri S. Modeling skin permeability to hydrophilic and hydrophobic solutes based on four permeation pathways. J Control Release. 2003;86(1):69–92.
29. Mak VHW, Potts RO, Guy RH. Does hydration affect intercellular lipid organization in the stratum corneum? Pharm Res. 1991;8(8):1064–5.
30. Warner RR, Stone KJ, Boissy YL. Hydration disrupts human stratum corneum ultrastructure. J Investig Dermatol. 2003;120(2):275–84.
31. Björklund S, Engblom J, Thuresson K, Sparr E. Glycerol and urea can be used to increase skin permeability in reduced hydration conditions. Eur J Pharm Sci. 2013;50(5):638–45.
32. Yousef S, Mohammed Y, Namjoshi S, Grice J, Sakran W, Roberts M. Mechanistic evaluation of hydration effects on the human epidermal permeation of salicylate esters. AAPS J. 2017;19(1):180–90.